Strain-gradient effects in nanoscale-engineered magnetoelectric materials

Aliona Nicolenco[1,2], Muireann de h-Óra[3], Chao Yun[3], Judith MacManus-Driscoll[3], *and* Jordi Sort[1,4]

[1]Departament de Física, Universitat Autònoma de Barcelona, 08193 Bellaterra, Spain

[2]Institute of Applied Physics, 2028 Chisinau, Moldova

[3]Department of Materials Science and Metallurgy, University of Cambridge, CB3 OFS Cambridge, United Kingdom

[4]Institució Catalana de Recerca i Estudis Avançats, Pg. Lluís Companys 23, 08010 Barcelona, Spain

ABSTRACT

Understanding strain gradient phenomena is of paramount importance in diverse areas of condensed matter physics. This effect is responsible for flexoelectricity in dielectric materials, and it plays a crucial role in the mechanical behavior of nanoscale-sized specimens. In magnetoelectric composites, which comprise piezoelectric or ferroelectric (FE) materials coupled to magnetostrictive (MS) phases, the strain gradient can add to any uniform strain that is present to boost the strength of the coupling. Hence, it could be advantageous to develop new types of functionally graded multiferroic composites (for information technologies) or magnetic-field-driven flexoelectric/magnetostrictive platforms for wireless neurons/muscle cell stimulation (in biomedicine). In MS or FE materials with non-fully constrained geometries (e.g., cantilevers, porous layers, or vertically aligned patterned films), strain gradients can be generated by applying a magnetic field (to MS phases) or an electric field (to, e.g., FE phases). While multiferroic composites operating using uniform strains have been extensively investigated in the past, examples of new nanoengineering strategies to achieve strain-gradient-mediated magnetoelectric effects that could ultimately lead to high flexomagnetoelectric effects are discussed in this Perspective.

I. INTRODUCTION

Magnetism and electricity have always had an intimate link. Particularly interesting is the coexistence of magnetic and electric orders in magnetoelectric (ME) materials, which makes them able to respond, simultaneously, to external magnetic and electric stimuli: (i) electric polarization can be modulated by the external magnetic field (*direct ME effect, DME*) and (ii) magnetic properties can be largely controlled with an electric field (*converse ME effect, CME*).[1] In conventional ME composites, the coupling between piezoelectric [or ferroelectric (FE)] and magnetostrictive (MS) constituents is mediated by homogeneous interfacial strain and, in some cases, by electric surface charge effects.[2,3] DME effects are appealing for healthcare technologies,[4] water remediation,[5] energy harvesting systems,[6] and sensors/actuators,[7] whereas CME effects can be exploited in microelectromechanical systems and to reduce energy consumption of magnetic memories and spintronic devices.[8]

The idea of using strain transfer to induce a coupling between FE and MS phases in multiferroic heterostructures dates back to 1972,[9] a few years after the intrinsic magnetoelectric effect had been experimentally demonstrated for the first time in single-phase Cr_2O_3[10] (see Fig. 1). During subsequent years, particulate composites, comprising either FE (e.g., $BaTiO_3$) or MS (e.g., $CoFe_2O_4$) particles,[11,12] were extensively studied for their potential applications. However, the weak ME coupling in multiferroics (single-phase and heterostructured) at room temperature and the high dielectric losses have hampered practical applications of these materials. During the 1990s, the interest in magnetoelectricity was revived again when a wide range of advanced experimental techniques for synthesis and characterization of nanomaterials became available [e.g., piezoresponse force microscopy, scanning transmission electron microscopy, and advanced pulsed laser deposition (PLD) techniques] that triggered new theoretical advances (e.g., development of a density-functional theory), allowing a better understanding of this phenomenon.

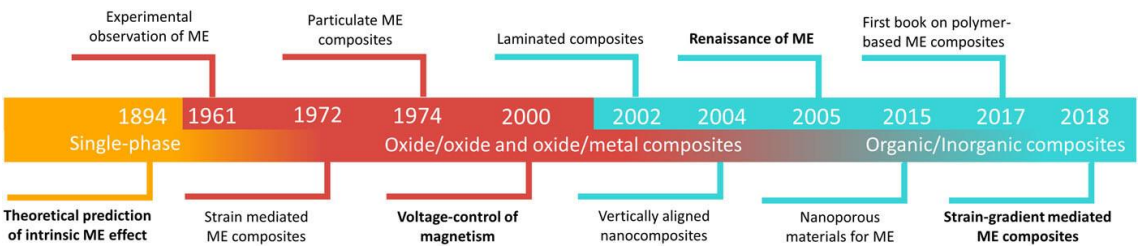

FIG. 1. Timeline illustrating the major milestones in the investigation of the ME effect.

A further leap in the field occurred in 2000 when the converse magnetoelectric effect, experimentally demonstrated by Ohno *et al.*[13] and Weisheit *et al.*,[14] was shown to be a suitable strategy to manipulate the magnetic properties of diluted semiconductors and ultra-thin metallic films with voltage. Concurrently, laminated composites based on new materials [e.g., Terfenol-D, Metglas or $Pb(Mg_{1/3}Nb_{2/3})O_3$–$PbTiO_3$] soon became available, leading to ME coupling coefficients tens of times larger than in particulate composites.[15] Then, two-phase, vertical nanocomposite/nanostructured films (VANs) began to be explored.[16] Many VAN reports have been made over the last nearly 20 years, with attention focused on the manipulation of vertical strain rather than lateral (horizontal) strain, which is the case for standard heterostructures,[17] and advances in micro-/nano-thin film technology, with atomic-scale control of the connectivity between the phases, have further contributed to the renaissance of magnetoelectricity.

During the last 20 years, a large increase in the number of publications and patents covering magnetoelectric effects in the areas of spintronics, memories, sensors, actuators, biomedical application, and many others has been observed (the number exceeds 20 000 according to the ISI Web of Science). Most of these works focus on conventional multiferroic composites (where the ME effects are mediated by homogeneous strain), magneto-ionics, or surface charge effects. The effects of strain gradients in ME heterostructures still remain rather unexplored (only around 50 publications during the last five years). Nanoporous materials,[18] polymer-based composites,[19] and VANs[20] constitute the most promising materials for strain-gradient engineered ME composites and require deeper exploration.

There are several challenges associated with the operation of conventional ME composites. In MS films directly grown onto FE substrates, the voltage required to generate ME effects is extremely high (e.g., 4 kV)[21] due to the large thickness of the substrate (i.e., in capacitors, the electric field is inversely proportional to the dielectric thickness). This is not suitable for microelectronics, where much lower voltages (<10 V) are desirable to enhance energy efficiency and not burn the electronic components. If thin FE/MS bilayers are directly grown onto rigid (non-FE) substrates, then the required voltages are lower, but the attainable strain is small due to the clamping with the substrate, thus also limiting ME effects.[22] The use of

flexible substrates can minimize this problem but high-quality FE/MS bilayers (specially containing oxide FE) are not easy to prepare on flexible substrates. To overcome the aforementioned challenges and thus to achieve large DME and CME effects with low applied voltages***, strain gradient effects*** in continuous (non-patterned) films grown on rigid substrates could be used while circumventing the problems of substrate clamping.

In contrast to conventional piezoelectricity where the change in polarization is induced by homogeneous strain, the gradient of strain ultimately leads to the "flexoelectric effect," which is universal for all dielectric materials.[23] The flexoelectric effect is proportional to the dielectric constant, and since FEs have very large dielectric constants, flexoelectricity is maximized for this class of materials. The flexoelectric coefficients in dielectrics have been measured to be in the range 10^{-4} μC/m–10^{-5} μC/m in elastomers,[24] 100 μC/m in piezoelectric $BaSrTiO_3$,[25] 287 μC/m–418 μC/m in FE $BaTiO_3$,[26] and even as high as 1000 μC/m in the oxygen-depleted $BaTiO_{3-\delta}$ semiconductor, $BTO_{-\delta}$.[27] Furthermore, there have been predictions that flexoelectricity should significantly enhance the piezoelectric performance at the nanoscale,[28,29] although direct evidence of this remains rather elusive due to the difficulties in generating strain gradients in conventional clamped thin films. At the surface of a film under a mechanical force of 0.1 μN, the effective piezoelectric coefficient, d^{eff}_{33}, has been shown to be an order of magnitude larger in flexoelectric $SrTiO_3$ than in piezoelectric quartz.[30] The flexoelectric effect diminishes with distance, r, from the mechanical tip-to-surface contact ($1/r^3$ for 3D geometries), hence the reason why flexoelectricity specifically dominates in thin films.[31]

In terms of the impact of flexoelectricity on magnetoelectric effects, there have been only a few experimental reports in the last few years of flexoelectricity combined with magnetism.[20,32,33] The state-of-the-art in the development of these strain-gradient-mediated magnetoelectric materials and future potential directions is discussed in this Perspective. Specifically, in Sec. II, we discuss mechanically induced strain gradient effects in FE and MS continuous layers that were traditionally studied separately and have not been combined yet to produce ME composites. In Sec. III, we then focus on the strain-gradient-mediated ME bilayers based on a mesoporous/nanoporous MS matrix partially filled with the FE phase that can be prepared to boost strain gradient effects. When grown onto rigid substrates, ME effects in such heterostructures are mediated by strain-gradients instead of homogeneous strain. The effect is enhanced in high-

aspect-ratio patterned elements, i.e., VANs, where clamping occurs only right at the bottom part of the structure, and so, lateral strains are developed along the vertical direction, as it is discussed in detail in Sec. IV. Finally, we provide an outlook for the possible application of the strain-gradient-mediated ME composites in Sec. V, and some general conclusions are given in Sec. VI.

II. MECHANICALLY INDUCED STRAIN GRADIENTS IN MAGNETOSTRICTIVE AND FERROELECTRIC MATERIALS

Strain gradients can be mechanically induced in bulk specimens or dense films by, for example, bending or nanoindentation. The highest possible strain gradients in materials with self-constrained (i.e., non-porous) geometries occur at the end of crack tips.[34] The interplay between flexoelectricity and fracture behavior has been studied in some detail in several oxide materials (including bone or FE compounds).[35,36] Crack-propagation in FE oxides can be either aided or obstructed by the orientation of the ferroelectric polarization. In other words, the strain-gradient at the tip of the crack induces a flexoelectric polarization either antiparallel or parallel to the ferroelectric polar axis, thereby resulting in asymmetric crack formation.[37]

In turn, the effects of nanoindentation strain gradients on the magnetic properties of some specific alloys (FeAl, FeRh, etc.) have also been investigated in detail. FeAl undergoes an order-disorder paramagnetic-to-ferromagnetic transition when subjected to plastic deformation at the atomic scale.[38] FeRh exhibits a metamagnetic transition (from the antiferromagnetic to ferromagnetic state) that can be also tuned by the strain gradient (i.e., a direct spatial correlation between the metamagnetic transition temperature of this alloy and local strain values has been recently reported).[39] The flexoelectric effects induced by nanoindentation in multiferroic materials could give rise to changes in the magnetic properties (i.e., to give flexomagnetism). The changes in the magnetic behavior of materials caused by inhomogeneous FE polarization have been sometimes referred to as flexomagnetoelectric effects.[40,41] These have been reported in certain single phase multiferroics, but their strength could be enhanced in suitably engineered composites (note that the strain-gradient effects in MS and FE materials so far have been mainly studied separately). In particular, one could try to control crack propagation as a means to tailor the performance of magnetoelectric devices to achieve an optimized CME.

III. STRAIN GRADIENTS IN MAGNETOELECTRIC COMPOSITES BASED ON MESOPOROUS AND NANOPOROUS MATERIALS

Mesoporous and nanoporous materials have recently attracted much attention for the fabrication of ME composites due to their ability to accommodate various guest materials.[42–44] It is worth mentioning that the vast majority of works deal with CME, where the changes in magnetic properties of the porous matrix are governed by electric surface charge accumulation or interface oxidation–reduction reactions.[3,18] Indeed, in these cases, the presence of pores brings about a drastic increase in the surface-to-volume ratio that significantly enhances ME effects. Only a few studies were focused on the strain-mediated ME composites based on porous materials.[43,45,46] This is probably due to several factors: (i) a high-quality interface should be created between the MS and FE phases to ensure effective transfer of strain, which may not be straightforward in the case of complex 3D porous structures; (ii) porous materials show complex magnetostrictive behavior that is difficult to predict (magnetostriction can either increase or decrease or remain unchanged dependently on the magnetostrictive constants and porosity degree) and sometimes even more difficult to measure;[47] (iii) for CME, the FE phase should not have electric pinholes (otherwise the electric charges are not accumulated to create the electric field), which sometimes may become a technological challenge. Nevertheless, MS meso-/nanoporous materials are excellent candidates to study the strain-gradient induced ME effects, as it is discussed hereafter.

An interesting example of this type of composite is the uniform deposition of piezoelectric lead zirconate titanate (PZT) into the templated mesoporous MS $CoFe_2O_4$ thin film for CME.[45] Out-of-plane (OOP) magnetic measurements of this system revealed that, contrary to expectations based on the total PZT volume fraction, mesoporous CFO samples partially filled with PZT showed larger changes in the magnetization than the sample with fully filled pores. The authors argued that the residual porosity in the composites added mechanical flexibility enabling greater ME coupling, which can be interpreted as a consequence of strain gradient effects. Similar results were also reported in mesoporous $BiFeO_3$ single-phase multiferroic on application of an electric field.[48]

Another recent example is the growth of porous FeGa MS layers by electrodeposition onto rigid Si/Cu substrates and the subsequent coating with the P(VDF-TrFE) FE polymer by spin coating.[49] Under the magnetic field (DME), the FeGa was found to be compressed, on average, by 0.033% [as evidenced by x-ray diffraction (XRD)]. The experimental results revealed that while the bottom of the FeGa layer remains clamped, its air side exhibits a pronounced tetragonal deformation, thanks to the residual nanoporosity existing between the columnar grains of the electrodeposited

films (see Fig. 2). It is worth mentioning that while the FE layer most likely experiences an homogeneous strain due to its relatively large thickness (strain-gradient effects are more pronounced at the nanoscale), the magnetic-field induced strain gradient in nanoporous FeGa causes a change in the piezoresponse of the adjacent ferroelectric P(VDF-TrFE) layer, as evidenced by piezo-response force microscopy.

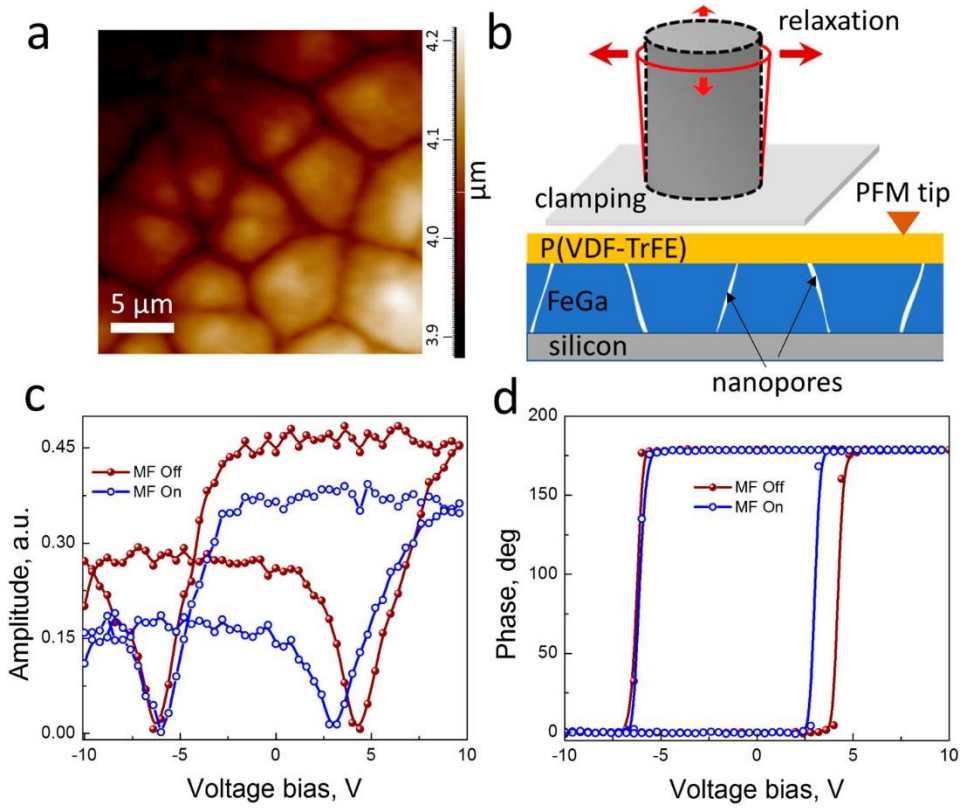

FIG. 2. Magnetoelectricity in a FeGa/P(VDF-TrFE) bilayer mediated by a strain gradient developed in the FeGa phase. (a) The topography image, (b) schematic illustration of the strain gradient development in each FeGa grain, (c) local piezo-response amplitude, and (d) phase loops obtained from the Fe–Ga/P(VDF-TrFE) heterostructure without (MF Off) and with (MF On) the application of a magnetic field of 0.1 T. Adapted from Ref. 49.

These works thus reveal that, owing to their high mechanical flexibility, nanoporous materials offer unique opportunities for the design of strain-gradient mediated ME structures. Specifically, MS porous matrices could be used to produce inorganic–organic composites by, e.g., infiltrating the FE polymers. Such heterostructures are expected to have a larger biocompatibility (see Sec. V for further details) due to the reduced Young's modulus of the porous metallic counterpart.[50] In addition, in high surface area composites, the flexoelectricity caused by inhomogeneous strain generated by each MS ligament can be added to piezoelectricity leading to an enhanced ME effect.

IV. STRAIN GRADIENTS IN VERTICALLY ALIGNED NANOCOMPOSITES

Strain coupling between piezoelectric and magnetostrictive materials in VAN systems has been widely explored over many years. There are two main types. The first type is made by chemical solution methods, which do not rely on epitaxial growth and where feature sizes are relatively large (>100 nm),[51] and the second type are VANs made by physical vapor deposition, with feature sizes of ∼10 nm–20 nm. Similar to the composites discussed in Sec. III above, these VAN systems are substrate anchored and hence have the potential for memory and sensor applications.

There are only a few experimental works of the chemical-method composite films that exploit the flexoelectric effect.[33,52,53] Flexoelectricity is combined with magnetostriction to produce vertically coupled ME composite materials. A notable example is the work of Poddar *et al.* who fabricated Ni matrix/P(VDF-TrFE) pillar films.[20] Periodic arrays of FE P(VDF-TrFE) square pillars (62 nm height and ∼185 nm lateral size) were obtained by nanoimprint lithography, and the MS Ni matrix was made by electrodeposition [Fig. 3(a)]. The Ni matrix was physically clamped to a rigid substrate. It was demonstrated that the polarization of the FE P(VDF-TrFE) can be locally switched by an external magnetic field applied to the composite due to transfer of inhomogeneous strain from the MS Ni matrix. The strain induced in the P(VDF-TrFE) pillars increased from the bottom to the top, producing a strain gradient (and hence the flexoelectric effect) along the z vertical axis. Finite element analysis demonstrated that as the distance from the substrate increases, the Ni matrix contracts (negative vertical displacement field, U_3), while the pillars experience a large expansion (positive U_3), as shown in Fig. 3(b). The strain in the pillars increased significantly with thickness [Fig. 3(c)]. From these data, the flexoelectrically generated electric field profile could be obtained [Fig. 3(d)]. Notably, the largest changes occurred within the first 20 nm from the substrate, which further supports that flexoelectric effects are more pronounced in features with very small dimensions.[23] Due to the strain gradient effects and the inhomogeneous ME coupling along the pillar length, the polarization direction of the P(VDF-TrFE) pillars could be reversed using magnetic fields.

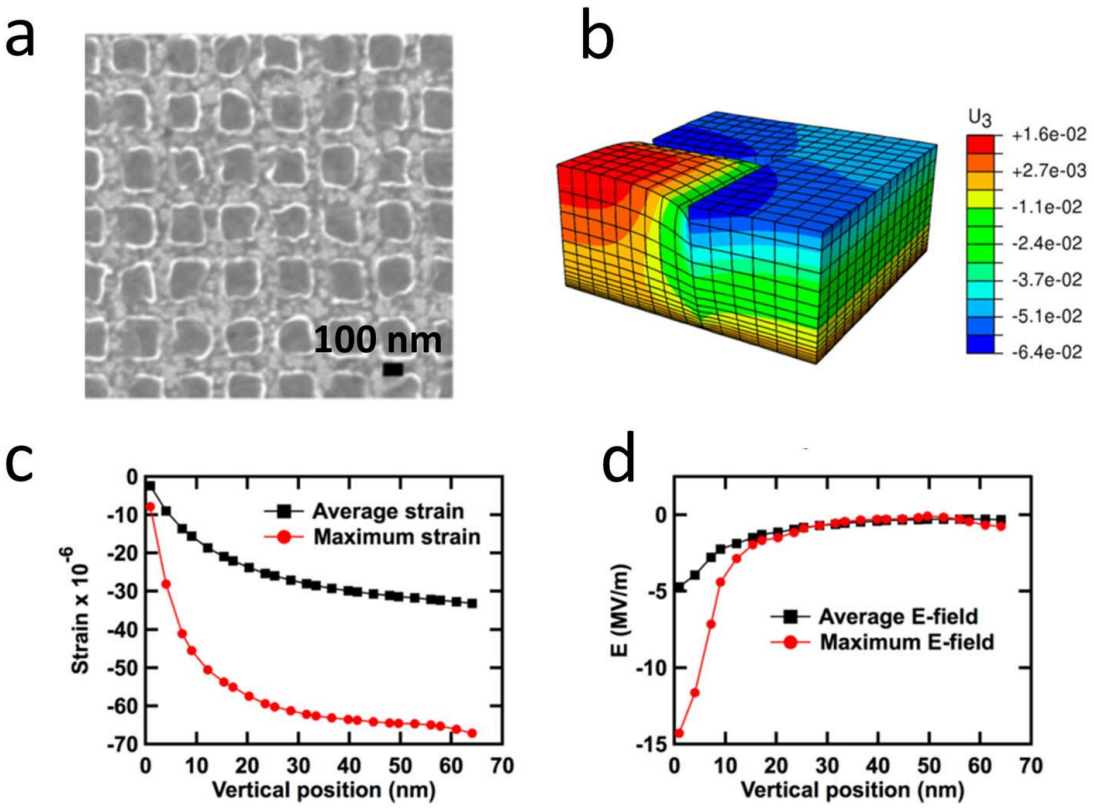

FIG. 3. Strain-gradient mediated Ni/P(VDF-TrFE) composite. (a) The SEM image of the heterostructure showing P(VDF-TrFE) nanopillars embedded in an electrodeposited Ni matrix. [(b)–(d)] Finite element analysis: (b) the vertical displacement field in the pillars and matrix normalized by the magnetostrictive strain, (c) average and maximum strains in the FE pillars along the vertical position, and (d) average and maximum strain-gradient-generated electric fields along the vertical position of the P(VDF-TrFE) pillar. Reprinted with the permission from Poddar *et al.*, ACS Nano **12**(1), 576–584 (2018). Copyright 2018. American Chemical Society.

Considering the physical vapor deposited systems, here ME effects in VAN films have been obtained in many systems incorporating FE (and hence piezoelectric) phases, such as $BaTiO_3$ or $BiFeO_3$, with MS systems ($CoFe_2O_4$ being the most common). The films are grown in the epitaxial form in a one step process by physical vapor deposition, and the VAN structure forms by self-assembly [schematic VAN structure shown in Fig. 4(a)]. Results for both the DME effect[54–59] and the CME effect[60] have been achieved. The ME coupling coefficients in such VAN structures are typically $\sim 10^{-9}$ s/m. Challenges for these systems are electrical leakage, and the need to apply a magnetic field to realize the maximum ME coupling effect, not only for DME but also CME.[60]

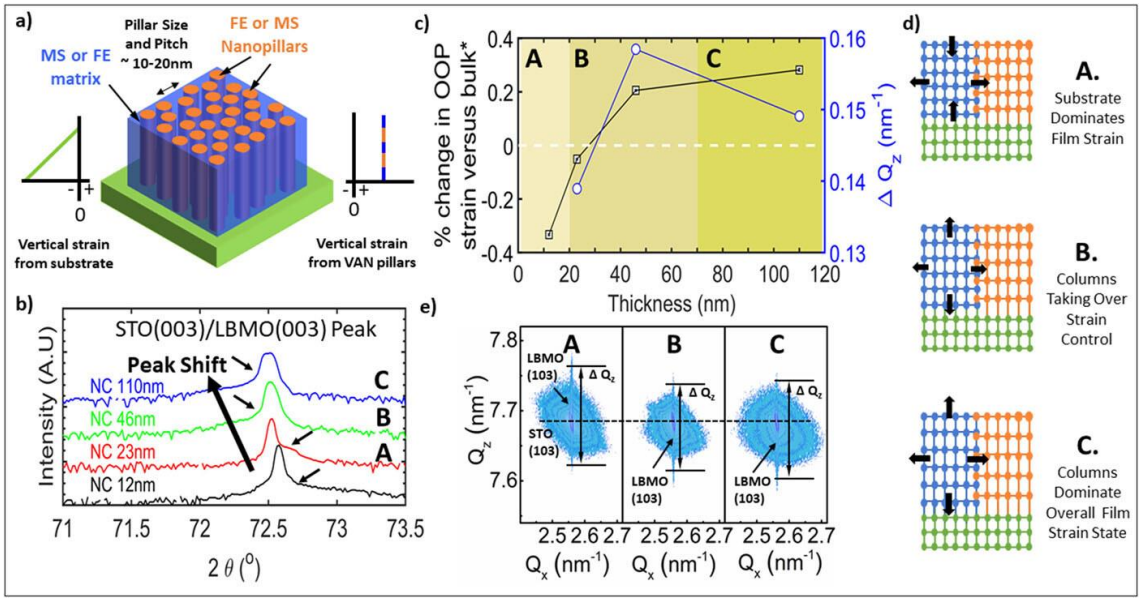

FIG. 4. One-step thin film process for inducing flexoelectricity via self-assembled vertically aligned nanocomposite (VAN) films. (a) The schematic of a VAN structure illustrating how vertical strain induced by the substrate relaxes as the film grows, whereas vertical strain induced by the vertical pillars stays constant. (b) The XRD plot for the exemplar system LBMO/CeO_2 showing the increasing vertical strain with film thickness, switching from substrate-controlled to pillar controlled strain. The arrows indicate the positions of the LBMO (003) film peaks that overlap the STO (003) peak. **(**c) The percentage change in out-of-plane (OOP) strain vs the bulk material, with increasing thickness across three different regions of A, B, and C. (d) The schematic of the average strain state in a VAN film cross section with increasing film thickness in regions A, B, and C. (e) X-ray reciprocal space maps of the LBMO (103) peak for different thickness films in regions A, B, and C. The reciprocal peak broadening along the out-of-plane direction is indicated on each plot, as ΔQ_z (a measure of the non-uniformity of the OOP strain) and the values are shown in (c).

As far as known, strain-gradient-mediated/flexoelectric-mediated magnetoelectricity has not been studied in these self-assembled VAN composites. However, there is much promise since VAN films have both vertical strain and thickness-dependent strain gradient effects. Hence, it should be possible to induce either a flexoelectric effect in a FE phase or a large strain gradient effect in a MS phase.

We consider in Fig. 4 a VAN film example from our earlier work where thickness-dependent strain and strain gradients have been measured.[61] The system is $La_{0.9}Ba_{0.1}MnO_3$ (LBMO, matrix)/CeO_2 (pillar) grown by pulsed laser deposition (PLD) from a composite target on single crystal $SrTiO_3$. The LBMO film is insulating, and based on the fact that FM 3d metals typically show MS behavior,[62] and insulating

$La_{0.8}Ba_{0.2}MnO_3$[63] shows a large MS effect and $La_{0.9}Ba_{0.1}MnO_3$ is also expected to be an MS phase. The CeO_2 is not, however, ferroelectric (it is an ionic conductor), and it is not possible to achieve a ME effect via strain coupling. On the other hand, the system of Fig. 4 simply serves to show the vertical strain effects in a typical VAN film.

There is not a limitation that the MS phase must be the matrix and the FE phase must be the pillars. Indeed, the opposite case has been more commonly studied (FE matrix and MS pillars).[64] For creating ME systems, both the FE and MS phases need to be near-insulating, otherwise leakage currents and Joule heating effects hamper device performance. The pillar phases are typically 10 nm–20 nm in diameter and of a similar pitch. This fine feature size ensures a huge vertical interfacial area for coupling effects with the matrix phase.

As shown in Fig. 4(a), the LBMO matrix phase (blue) has nanopillars of CeO_2 (orange) grown within it, and the whole film is supported on the substrate (green). To achieve good quality epitaxy and a clear phase separated structure, the films were grown at ~700 °C. More generally, for VAN films to achieve epitaxy, the films need to be grown above ~600 °C, the actual temperature depending on the specific cations in the composite PLD target. Of all crystalline materials that can be deposited, the perovskite materials are grown most perfectly as a matrix in epitaxial film form on the most commonly available substrates, i.e., perovskites. The pillars that grow within the matrix are typically not perovskite structured; otherwise, intermixing with the matrix is likely to occur.

VAN films offer very interesting strain effects that cannot be achieved in plain, single phase epitaxial films.[65,66] This is because of the presence of vertical epitaxy between the pillars and the matrix, which is additive to the epitaxy of the matrix phase with the substrate. Hence, there are 3D epitaxial effects. For very thin films, substrate epitaxy dominates, but this strain relaxes as the film grows. The variable substrate strain effect and constant VAN pillar strain effect are shown schematically in Fig. 4(a) on the left hand and right hand of the film schematic. If two vertical strain components are added, it is clear that the strain in the largest film thicknesses is influenced only by the pillar effect. This is manifested in the XRD plots of Fig. 4(b). Hence, the substrate diminishes with increasing film thickness.

We see that the LBMO (003) peak [indicated by arrows in Fig. 4(b)] moves from the right-hand side of the STO (003) substrate peak (lattice parameter 3.905 Å) to its left as the film thickens, indicating an increasing out-of-plane (OOP) lattice parameter. As expected, the STO will tense the LBMO in-plane (LBMO bulk lattice parameter is ~3.875 Å,[67] depending on the precise composition[68]), leading to compression OOP (from Poisson effects) that relaxes with film thickness. Hence, the LBMO film OOP lattice compresses less with film thickness and, in fact, goes into tension. This is shown in Fig. 4(c). The white dashed line shows approximately the position of switchover from compression to tension. We can label three different regions of [Fig. 4(c)], A, B, and C. These same regions are also shown in Fig. 4(b).

Region A is where epitaxy with the substrate dominates the OOP lattice parameter, B is the mixed region where vertical epitaxy with the nanopillars begins to play a strong role in controlling the OOP strain but where substrate effects are not negligible, and C is the region where the nanopillars dominate the OOP strain in the upper part of film that is from the substrate. Here, the OOP lattice parameter is close to saturation for the vertical strain level that the pillars can provide. For this system, the OOP strain level for the thickest film is ~0.3%. In fact, it is possible to achieve >1% strains in other perovskite VAN systems, e.g., $BaTiO_3$-based.[69–71]

Figure 4(d) shows schematically the *average* strain state schematically in a VAN film cross section with increasing film thickness. Considering that OOP strain is compresive for very thin films and tensile for thick films, there will be a gradient of strain in the relatively thick structures, progressing from compressive to tensile, as the distance from the rigid substrate increases. X-ray reciprocal space maps of the LBMO (103) peak for different thickness films in regions A, B, and C [Fig. 4(e)] were used to assess the variation in strain (or level of non-uniformity of strain) in the OOP direction (from the FWHM of the reciprocal space peak along the z (OOP) direction), i.e., ΔQ_z and the values are shown as a function of thickness in Fig. 4(c). In region B (film thickness 46 nm), ΔQ_z shows a maximum value consistent with the largest mix of strain values in the transition region from substrate to pillar control, i.e., from OOP compression to OOP tension. In region C [largest thickness film (110 nm)], most of the film is in tension OOP and is pillar dominated and so is more uniform, and so, ΔQ_z decreases, cf. region B. Overall, a 110 nm thick film can provide a large strain gradient effect.

For the VAN example given here, the OOP strain value changes from −0.3% at the bottom of the film to +0.3% at the top, i.e., 0.6% difference, but as already mentioned, strain gradients of over 1% are possible, depending on the specific materials in the VAN film. Hence, although not studied for inducing strain gradient effects, there is a strong potential for VAN to achieve either a strain-gradient flexoelectric effect in the FE material to achieve enhanced polarization or to achieve a large strain gradient in the MS material to achieve enhanced MS. Both effects should lead to enhanced ME coupling.

V. BEYOND CONVENTIONAL PIEZOELECTRIC-MAGNETOSTRICTIVE COMPOSITES

In the recent years, stain-gradient effects have been studied in various MS magnetic and FE materials, leading to interesting effects such as flexomagnetism and flexoelectricity. However, there are only a few systems where the strain gradients were studied in coupled MS/FE systems, i.e., in ME composites. Compared to the conventional strain mediated ME systems where the effects are mediated by homogeneous strain, the inhomogeneous strain can significantly enhance the performance of the composite films at the nanoscale, when the features size falls below ∼50 nm. Interestingly, this could render functionally graded materials (with tunable ME properties along the vertical direction), which are not possible to obtain using conventional ME approaches. This opens up a new range of possibilities for the utilization of strain-gradient mediated ME composites. Specifically, two main applications of such materials can be envisaged.

A. Strain-graded ME composites for biomedical applications (DME)

Wireless, non-invasive electric stimulation of living cells (without implanted electrodes) is of paramount interest in biomedicine.[72,73] Several studies (including *in vivo* tests)[74] have shown that ME core–shell nanoobjects, e.g., FeGa/P(VDF-TrFE) or $CoFe_2O_4/BaTiO_3$ nanoparticles, can generate reasonable electric fields (∼1 kV/m), allowing optimum conversion from magnetic to electric energy for minimally invasive localized treatments.[4,74] In ME composites, by adding the effect of the strain gradient to the effect of strain itself, i.e., adding flexoelectricity to piezoelectricity, the attainable electrical polarization induced by magnetic fields can be largely enhanced.[23] In fact, the inherent flexoelectricity of bone has been reported to play a central role in bone-crack self-repair.[35] However, DME

combining flexoelectricity with magnetostriction has been largely unexploited. Nonetheless, it has been recently reported that the polarization in flexoelectric MS/FE heterostructures can be directly switched with an external magnetic field.[20] This is generally not possible using only piezoelectric/magnetostrictive composites. The possibility to locally switch polarization in some regions of the material while preserving the original polarization direction in the others is related to local strain gradients, and it opens new avenues for tissue engineering applications, where magnetic fields (and magnetic field gradients) with different strengths and signs could allow tailoring cell proliferation in different regions or directions at different rates, depending on the locally induced variations of the electric polarization.

B. Strain-graded ME composites for energy-efficient information technologies (CME)

In magnetic storage devices and memories, the CME effect is used to reduce the coercivity (H_C) of the media so that the information can be stored under lower applied magnetic fields (which means using lower electric currents, thereby reducing Joule heating effects).[8] In archetypical ME memories, each memory unit (bit) behaves as a "single entity" with a single set of homogeneous properties.[75] Functionally graded magnetic materials, in which there is a gradual variation of properties (e.g., H_C) across the thickness of the memory unit, emerged as an interesting class of materials to write information with lower magnetic fields (also improving the signal-to-noise ratio) while still guaranteeing stability of the media, thanks to the counterpart that retains a large coercivity.[76,77] In conventional functionally graded magnetic materials, the composition of the layers is progressively varied through the film thickness by, e.g., doping with non-magnetic elements (e.g., by diluting FePt with Cu).[76] However, after fabrication, each memory unit prepared in this way exhibits a unique (fixed) range of properties that is determined by the gradient in composition. Strain gradients could be used as a new strategy to surpass conventional functionally graded magnetic materials in which tunable ME effects will be induced in FE/MS clamped heterostructures by means of the strain gradient. Hence, a wide range of H_C values could be obtained in this way from each single memory unit (with a unique homogeneous composition) by simply varying the strength of the applied voltage. During the process of writing, the spins will be aligned in the same direction throughout the film

thickness (from top to bottom) due to the exchange interactions. Suitable voltages should be selected to achieve maximum reduction in coercivity so that information can be written with low applied magnetic fields (low electric currents and minimizing power dissipation by the Joule heating effect).[78] As flexoelectric effects are inversely proportional to the features' size, i.e., "bits" size, larger effects are anticipated at the nanoscale. This is appealing for high density magnetic recording media.

VI. CONCLUSIONS

The development of new nanoengineered FE/MS composites of different sorts, such as partially filled mesoporous films or vertically aligned nanocomposite (VAN) structures, with the potential to exhibit large strain gradient effects, is likely to enhance currently available magnetoelectric phenomena for the holy grail of high performance DME or CME devices. The proper integration of strain gradients in this type of materials could result in voltage-driven functionally graded materials or in the reversal of electric polarization with magnetic fields or the analogous effects, i.e., the reversal of magnetization with voltage. Hence, flexomagnetoelectric materials and devices, governed by inhomogeneous strains, are appealing candidates for the investigation and implementation in the near future. The range of applications of these materials could extend beyond information technologies. For instance, their integration in the biomedical field could revolutionize current technologies for cell stimulation, prompting the development of wireless electrostimulation of neurons or chemotherapies (e.g., electric-field-driven drug delivery), among others. Despite intensive recent research efforts, this field remains still in its infancy and its potential is still to be demonstrated. Nevertheless, there are promising new avenues to follow, as outlined in this Perspective.

ACKNOWLEDGMENTS

This project has received funding from the European Union's Horizon 2020 research and innovation program under the Marie Sklodowska-Curie Grant Agreement No. 892661–MAGNUS. Financial support by the European Commission (BeMAGIC H2020-MSCA-ITN-2019 No. 861145 project), the European Research Council [SPIN-PORICS 2014-Consolidator Grant (No. 648454) and MAGIC-SWITCH 2019-Proof of Concept Grant (No. 875018)], the Spanish Government (MAT2017-86357-C3-1-R and associated FEDER),

and the Generalitat de Catalunya (Grant Nos. 2017-SGR-292 and 2018-LLAV-00032) is also acknowledged. J.M.M.-D. acknowledges support from the Royal Academy of Engineering—CIET1819_24, the Leverhulme Trust Grant No. RPG-2015-017, EPSRC Grant Nos. EP/N004272/1, EP/T012218/1, EP/P007767/1, and EP/M000524/1, and the Isaac Newton Trust in Cambridge [minute 16.24(p) and RG96474].

REFERENCES

1. 1.Y. Wang, J. Hu, Y. Lin, and C.-W. Nan, NPG Asia Mater. **2**, 61 (2010). https://doi.org/10.1038/asiamat.2010.32, **Google ScholarCrossref**
2. 2.A. Molinari, H. Hahn, and R. Kruk, Adv. Mater. **31**, 1806662 (2019). https://doi.org/10.1002/adma.201806662, **Google ScholarCrossref**
3. 3.C. Navarro-Senent, A. Quintana, E. Menéndez, E. Pellicer, and J. Sort, APL Mater. **7**, 030701 (2019). https://doi.org/10.1063/1.5080284, **Google ScholarScitation**, **ISI**
4. 4.X.-Z. Chen, M. Hoop, N. Shamsudhin, T. Huang, B. Özkale, Q. Li, E. Siringil, F. Mushtaq, L. Di Tizio, B. J. Nelson, and S. Pané, Adv. Mater. **29**, 1605458 (2017). https://doi.org/10.1002/adma.201605458, **Google ScholarCrossref**
5. 5.F. Mushtaq, X. Chen, H. Torlakcik, C. Steuer, M. Hoop, E. C. Siringil, X. Marti, G. Limburg, P. Stipp, B. J. Nelson, and S. Pané, Adv. Mater. **31**, 1901378 (2019). https://doi.org/10.1002/adma.201901378, **Google ScholarCrossref**
6. 6.V. Annapureddy, H. Palneedi, G.-T. Hwang, M. Peddigari, D.-Y. Jeong, W.-H. Yoon, K.-H. Kim, and J. Ryu, Sustainable Energy Fuels **1**, 2039 (2017). https://doi.org/10.1039/c7se00403f, **Google ScholarCrossref**
7. 7.Y. Wang, J. Li, and D. Viehland, Mater. Today **17**, 269 (2014). https://doi.org/10.1016/j.mattod.2014.05.004, **Google ScholarCrossref**
8. 8.J.-M. Hu and C.-W. Nan, APL Mater. **7**, 080905 (2019). https://doi.org/10.1063/1.5112089, **Google ScholarScitation**, **ISI**

9. 9.J. V. Suchtelen, Philips Res. Rep. **27**, 28 (1972). **Google Scholar**
10. 10.D. N. Astrov, Soviet Phys. - JETP **11**, 708 (1960). **Google Scholar**
11. 11.M. Satyam, K. Ramkumar, and D. B. Ghare, IETE Tech. Rev. **2**, 79 (1985). https://doi.org/10.1080/02564602.1985.11437731, **Google ScholarCrossref**
12. 12.C.-W. Nan, Phys. Rev. B **50**, 6082 (1994). https://doi.org/10.1103/physrevb.50.6082, **Google ScholarCrossref**
13. 13.H. Ohno, D. Chiba, F. Matsukura, T. Omiya, E. Abe, T. Dietl, Y. Ohno, and K. Ohtani, Nature **408**, 944 (2000). https://doi.org/10.1038/35050040, **Google ScholarCrossref**
14. 14.M. Weisheit, S. Fähler, A. Marty, Y. Souche, C. Poinsignon, and D. Givord, Science **315**, 349 (2007). https://doi.org/10.1126/science.1136629, **Google ScholarCrossref**
15. 15.J. Ryu, A. V. Carazo, K. Uchino, and H.-E. Kim, Jpn. J. Appl. Phys. **40**, 4948 (2001). https://doi.org/10.1143/jjap.40.4948, **Google ScholarCrossref**
16. 16.O. I. Lebedev, J. Verbeeck, G. Van Tendeloo, O. Shapoval, A. Belenchuk, V. Moshnyaga, B. Damashcke, and K. Samwer, Phys. Rev. B **66**, 104421 (2002). https://doi.org/10.1103/physrevb.66.104421, **Google ScholarCrossref**
17. 17.A. Chen, Y. Dai, A. Eshghinejad, Z. Liu, Z. Wang, J. Bowlan, E. Knall, L. Civale, J. L. MacManus-Driscoll, A. J. Taylor, R. P. Prasankumar, T. Lookman, J. Li, D. Yarotski, and Q. Jia, Adv. Sci. **6**, 1901000 (2019). https://doi.org/10.1002/advs.201901000, **Google ScholarCrossref**
18. 18.A. Nicolenco, C. Navarro-Senent, and J. Sort, "Nanoporous composites with converse magnetoelectric effects for energy-efficient applications," in *Reference Modules in Materials Science and Material Engineering* (Elsevier, 2021). p. 1. **Google ScholarCrossref**
19. 19.P. Martins and S. Lanceros-Méndez, Appl. Mater. Today **15**, 558 (2019). https://doi.org/10.1016/j.apmt.2019.04.004, **Google ScholarCrossref**
20. 20.S. Poddar, P. De Sa, R. Cai, L. Delannay, B. Nysten, L. Piraux, and A. M. Jonas, ACS Nano **12**, 576 (2018). https://doi.org/10.1021/acsnano.7b07389, **Google ScholarCrossref**

21.21.H. Ahmad, J. Atulasimha, and S. Bandyopadhyay, Sci. Rep. **5**, 18264 (2015). https://doi.org/10.1038/srep18264, **Google ScholarCrossref**
22.22.R. N. Torah, S. P. Beeby, and N. M. White, J. Phys. D: Appl. Phys. **37**, 1074 (2004). https://doi.org/10.1088/0022-3727/37/7/019, **Google ScholarCrossref**
23.23.P. Zubko, G. Catalan, and A. K. Tagantsev, Annu. Rev. Mater. Res. **43**, 387 (2013). https://doi.org/10.1146/annurev-matsci-071312-121634, **Google ScholarCrossref**
24.24.M. Marvan and A. Havránek, *Relationships of Polymeric Structure and Properties* (Steinkopff, 1988), Vol. 78, p. 33. **Google ScholarCrossref**
25.25.W. Ma and L. E. Cross, Appl. Phys. Lett. **81**, 3440 (2002). https://doi.org/10.1063/1.1518559, **Google ScholarScitation**, **ISI**
26.26.S. Huang, H.-M. Yau, H. Yu, L. Qi, F. So, J.-Y. Dai, and X. Jiang, AIP Adv. **8**, 065321 (2018). https://doi.org/10.1063/1.5031162, **Google ScholarScitation**, **ISI**
27.27.J. Narvaez, F. Vasquez-Sancho, and G. Catalan, Nature **538**, 219 (2016). https://doi.org/10.1038/nature19761, **Google ScholarCrossref**
28.28.C. Zhang, L. Zhang, X. Shen, and W. Chen, J. Appl. Phys. **119**, 134102 (2016). https://doi.org/10.1063/1.4945107, **Google ScholarScitation**, **ISI**
29.29.H. T. Chen and A. K. Soh, J. Appl. Phys. **112**, 074104 (2012). https://doi.org/10.1063/1.4757013, **Google ScholarScitation**, **ISI**
30.30.A. Abdollahi, N. Domingo, I. Arias, and G. Catalan, Nat. Commun. **10**, 1266 (2019). https://doi.org/10.1038/s41467-019-09266-y, **Google ScholarCrossref**
31.31.J. M. Gregg, Science **336**, 41 (2012). https://doi.org/10.1126/science.1220827, **Google ScholarCrossref**
32.32.Q. Pan, C. Fang, H. Luo, and B. Chu, J. Eur. Ceram. Soc. **39**, 1057 (2019). https://doi.org/10.1016/j.jeurceramsoc.2018.12.045, **Google ScholarCrossref**
33.33.R. Cai, V.-A. Antohe, Z. Hu, B. Nysten, L. Piraux, and A. M. Jonas, Adv. Mater. **29**, 1604604 (2017). https://doi.org/10.1002/adma.201604604, **Google ScholarCrossref**

34.34.H. Wang, X. Jiang, Y. Wang, R. W. Stark, P. A. Van Aken, J. Mannhart, and H. Boschker, Nano Lett. **20**, 88 (2020). https://doi.org/10.1021/acs.nanolett.9b03176, **Google ScholarCrossref**
35.35.F. Vasquez-Sancho, A. Abdollahi, D. Damjanovic, and G. Catalan, Adv. Mater. **30**, 1705316 (2018). https://doi.org/10.1002/adma.201705316, **Google ScholarCrossref**
36.36.K. Cordero-Edwards, N. Domingo, A. Abdollahi, J. Sort, and G. Catalan, Adv. Mater. **29**, 1702210 (2017). https://doi.org/10.1002/adma.201770269, **Google ScholarCrossref**
37.37.K. Cordero-Edwards, H. Kianirad, C. Canalias, J. Sort, and G. Catalan, Phys. Rev. Lett. **122**, 135502 (2019). https://doi.org/10.1103/physrevlett.122.135502, **Google ScholarCrossref**
38.38.J. Sort, A. Concustell, E. Menéndez, S. Suriñach, K. V. Rao, S. C. Deevi, M. D. Baró, and J. Nogués, Adv. Mater. **18**, 1717 (2006). https://doi.org/10.1002/adma.200600260, **Google ScholarCrossref**
39.39.M. Foerster, E. Menéndez, E. Coy, A. Quintana, C. Gómez-Olivella, D. Esqué de los Ojos, O. Vallcorba, C. Frontera, L. Aballe, J. Nogués, J. Sort, and I. Fina, Mater. Horizons **7**, 2056 (2020). https://doi.org/10.1039/d0mh00601g, **Google ScholarCrossref**
40.40.A. P. Pyatakov and A. K. Zvezdin, Eur. Phys. J. B **71**, 419 (2009). https://doi.org/10.1140/epjb/e2009-00281-5, **Google ScholarCrossref**
41.41.R. M. Vakhitov, Z. V. Gareeva, R. V. Solonetsky, and F. A. Mazhitova, Phys. Solid State **61**, 1043 (2019). https://doi.org/10.1134/s106378341906026x, **Google ScholarCrossref**
42.42.T. E. Quickel, V. H. Le, T. Brezesinski, and S. H. Tolbert, Nano Lett. **10**, 2982 (2010). https://doi.org/10.1021/nl1014266, **Google ScholarCrossref**
43.43.P. Martins, R. Gonçalves, A. C. Lopes, E. Venkata Ramana, S. K. Mendiratta, and S. Lanceros-Mendez, J. Magn. Magn. Mater. **396**, 237 (2015). https://doi.org/10.1016/j.jmmm.2015.08.041, **Google ScholarCrossref**

44.44.E. Dislaki, S. Robbennolt, M. Campoy-Quiles, J. Nogués, E. Pellicer, and J. Sort, Adv. Sci. **5**, 1800499 (2018). https://doi.org/10.1002/advs.201800499, **Google ScholarCrossref**
45.45.D. Chien, A. N. Buditama, L. T. Schelhas, H. Y. Kang, S. Robbennolt, J. P. Chang, and S. H. Tolbert, Appl. Phys. Lett. **109**, 112904 (2016). https://doi.org/10.1063/1.4962536, **Google ScholarScitation**, **ISI**
46.46.F. Mushtaq, H. Torlakcik, Q. Vallmajo-Martin, E. C. Siringil, J. Zhang, C. Röhrig, Y. Shen, Y. Yu, X.-Z. Chen, R. Müller, B. J. Nelson, and S. Pané, Appl. Mater. Today **16**, 290 (2019). https://doi.org/10.1016/j.apmt.2019.06.004, **Google ScholarCrossref**
47.47.C.-W. Nan, Y. Huang, and G. J. Weng, J. Appl. Phys. **88**, 339 (2000). https://doi.org/10.1063/1.373664, **Google ScholarScitation**, **ISI**
48.48.T. E. Quickel, L. T. Schelhas, R. A. Farrell, N. Petkov, V. H. Le, and S. H. Tolbert, Nat. Commun. **6**, 6562 (2015). https://doi.org/10.1038/ncomms7562, **Google ScholarCrossref**
49.49.A. Nicolenco, A. Gómez, X.-Z. Chen, E. Menéndez, J. Fornell, S. Pané, E. Pellicer, and J. Sort, Appl. Mater. Today **19**, 100579 (2020). https://doi.org/10.1016/j.apmt.2020.100579, **Google ScholarCrossref**
50.50.G. Ryan, A. Pandit, and D. Apatsidis, Biomaterials **27**, 2651 (2006). https://doi.org/10.1016/j.biomaterials.2005.12.002, **Google ScholarCrossref**
51.51.N. Ortega, A. Kumar, J. F. Scott, and R. S. Katiyar, J. Phys.: Condens. Matter **27**, 504002 (2015). https://doi.org/10.1088/0953-8984/27/50/504002, **Google ScholarCrossref**
52.52.R. Cai, V. A. Antohe, B. Nysten, L. Piraux, and A. M. Jonas, Adv. Funct. Mater. **30**, 1910371 (2020). https://doi.org/10.1002/adfm.201910371, **Google ScholarCrossref**
53.53.W. Dong, J. Liu, S. Li, K. Bi, M. Gu, H. Yuan, and Y. Luo, Ceram. Int. **46**, 25164 (2020). https://doi.org/10.1016/j.ceramint.2020.06.304, **Google ScholarCrossref**
54.54.H. Zheng, J. Wang, S. E. Lofland, Z. Ma, L. Mohaddes-Ardabili, T. Zhao, L. Salamanca-Riba, S. R. Shinde, S. B. Ogale, F. Bai, D.

Viehland, Y. Jia, D. G. Schlom, M. Wuttig, A. Roytburd, and R. Ramesh, Science **303**, 661 (2004). https://doi.org/10.1126/science.1094207, **Google ScholarCrossref**

55.55.A. Chen, Z. Bi, Q. Jia, J. L. Macmanus-Driscoll, and H. Wang, Acta Mater. **61**, 2783 (2013). https://doi.org/10.1016/j.actamat.2012.09.072, **Google ScholarCrossref**

56.56.N. Dix, R. Muralidharan, J.-M. Rebled, S. Estradé, F. Peiró, M. Varela, J. Fontcuberta, and F. Sánchez, ACS Nano **4**, 4955 (2010). https://doi.org/10.1021/nn101546r, **Google ScholarCrossref**

57.57.M. Lorenz, V. Lazenka, P. Schwinkendorf, F. Bern, M. Ziese, H. Modarresi, A. Volodin, M. J. Van Bael, K. Temst, A. Vantomme, and M. Grundmann, J. Phys. D: Appl. Phys. **47**, 135303 (2014). https://doi.org/10.1088/0022-3727/47/13/135303, **Google ScholarCrossref**

58.58.R. Muralidharan, N. Dix, V. Skumryev, M. Varela, F. Sánchez, and J. Fontcuberta, J. Appl. Phys. **103**, 07E301 (2008). https://doi.org/10.1063/1.2832346, **Google ScholarScitation**, **ISI**

59.59.F. Zavaliche, H. Zheng, L. Mohaddes-Ardabili, S. Y. Yang, Q. Zhan, P. Shafer, E. Reilly, R. Chopdekar, Y. Jia, P. Wright, D. G. Schlom, Y. Suzuki, and R. Ramesh, Nano Lett. **5**, 1793 (2005). https://doi.org/10.1021/nl051406i, **Google ScholarCrossref**

60.60.R. Wu, A. Kursumovic, X. Gao, C. Yun, M. E. Vickers, H. Wang, S. Cho, and J. L. Macmanus-Driscoll, ACS Appl. Mater. Interfaces **10**, 18237 (2018). https://doi.org/10.1021/acsami.8b03837, **Google ScholarCrossref**

61.61.C. Yun, E.-M. Choi, W. Li, X. Sun, T. Maity, R. Wu, J. Jian, S. Xue, S. Cho, H. Wang, and J. L. MacManus-Driscoll, Nanoscale **12**, 9255 (2020). https://doi.org/10.1039/c9nr08373a, **Google ScholarCrossref**

62.62.B. Kundys and H. Szymczak, Phys. Status Solidi A **201**, 3247 (2004). https://doi.org/10.1002/pssa.200405427, **Google ScholarCrossref**

63.63.R. V. Demin, L. I. Koroleva, R. V. Privezentsev, and N. A. Kozlovskaya, Phys. Lett. A **325**, 426 (2004). https://doi.org/10.1016/j.physleta.2004.03.077, **Google ScholarCrossref**

64.64.H. Zheng, J. Wang, L. Mohaddes-Ardabili, M. Wuttig, L. Salamanca-Riba, D. G. Schlom, and R. Ramesh, Appl. Phys. Lett. **85**, 2035 (2004). https://doi.org/10.1063/1.1786653, **Google ScholarScitation**, **ISI**
65.65.J. MacManus-Driscoll, A. Suwardi, A. Kursumovic, Z. Bi, C.-F. Tsai, H. Wang, Q. Jia, and O. J. Lee, APL Mater. **3**, 062507 (2015). https://doi.org/10.1063/1.4919059, **Google ScholarScitation**, **ISI**
66.66.J. L. MacManus-Driscoll, A. Suwardi, and H. Wang, MRS Bull. **40**, 933 (2015). https://doi.org/10.1557/mrs.2015.258, **Google ScholarCrossref**
67.67.J. Zhang, H. Tanaka, T. Kanki, J.-H. Choi, and T. Kawai, Phys. Rev. B **64**, 184404 (2001). https://doi.org/10.1103/physrevb.64.184404, **Google ScholarCrossref**
68.68.J. Wang, F. X. Hu, L. Chen, J. R. Sun, and B. G. Shen, J. Appl. Phys. **109**, 07D715 (2011). https://doi.org/10.1063/1.3545805, **Google ScholarScitation**
69.69.S. A. Harrington, J. Zhai, S. Denev, V. Gopalan, H. Wang, Z. Bi, S. A. T. Redfern, S.-H. Baek, C. W. Bark, C.-B. Eom, Q. Jia, M. E. Vickers, and J. L. MacManus-Driscoll, Nat. Nanotechnol. **6**, 491 (2011). https://doi.org/10.1038/nnano.2011.98, **Google ScholarCrossref**
70.70.O. Lee, S. A. Harrington, A. Kursumovic, E. Defay, H. Wang, Z. Bi, C.-F. Tsai, L. Yan, Q. Jia, and J. L. MacManus-Driscoll, Nano Lett. **12**, 4311 (2012). https://doi.org/10.1021/nl302032u, **Google ScholarCrossref**
71.71.A. Kursumovic, E. Defay, O. J. Lee, C. F. Tsai, Z. Bi, H. Wang, and J. L. MacManus-Driscoll, Adv. Funct. Mater. **23**, 5881 (2013). https://doi.org/10.1002/adfm.201300899, **Google ScholarCrossref**
72.72.G. Murillo, A. Blanquer, C. Vargas-Estevez, L. Barrios, E. Ibáñez, C. Nogués, and J. Esteve, Adv. Mater. **29**, 1605048 (2017). https://doi.org/10.1002/adma.201605048, **Google ScholarCrossref**
73.73.M. Hoop, X.-Z. Chen, A. Ferrari, F. Mushtaq, G. Ghazaryan, T. Tervoort, D. Poulikakos, B. Nelson, and S. Pané, Sci. Rep. **7**, 4028 (2017). https://doi.org/10.1038/s41598-017-03992-3, **Google ScholarCrossref**

74.74.A. Rodzinski, R. Guduru, P. Liang, A. Hadjikhani, T. Stewart, E. Stimphil, C. Runowicz, R. Cote, N. Altman, R. Datar, and S. Khizroev, Sci. Rep. **6**, 20867 (2016). https://doi.org/10.1038/srep20867, **Google ScholarCrossref**
75.75.J. Cui, J. L. Hockel, P. K. Nordeen, D. M. Pisani, C.-Y. Liang, G. P. Carman, and C. S. Lynch, Appl. Phys. Lett. **103**, 232905 (2013). https://doi.org/10.1063/1.4838216, **Google ScholarScitation**
76.76.C. L. Zha, R. K. Dumas, Y. Y. Fang, V. Bonanni, J. Nogués, and J. Åkerman, Appl. Phys. Lett. **97**, 182504 (2010). https://doi.org/10.1063/1.3505521, **Google ScholarScitation**, **ISI**
77.77.V. M. Petrov and G. Srinivasan, Phys. Rev. B **78**, 184421 (2008). https://doi.org/10.1103/PhysRevB.78.184421, **Google ScholarCrossref**
78. 78.E. Menéndez, V. Sireus, A. Quintana, I. Fina, B. Casals, R. Cichelero, M. Kataja, M. Stengel, G. Herranz, G. Catalán, M. D. Baró, S. Suriñach, and J. Sort, Phys. Rev. Appl. **12**, 014041 (2019). https://doi.org/10.1103/physrevapplied.12.014041, **Google ScholarCrossref**